Polymer Chemistry

Accepted Manuscript

ROYAL SOCIETY OF CHEMISTRY

www.rsc.org/polymers

Facile green ring-opening polymerization of L-lactide catalyzed by natural kaoline

Jie Gao,[a] Feng Bao,*[a] Duo Wang,[b] Rui Ma,*[b] Sanfeng Jiang,[a] Xu Zhang,[a] Yanjin Yao,[a] Xiaobing Han[a] and Chunjie Yan[b]

[a] *College of Chemistry, Central China Normal University, Wuhan, 430079, China. E-mail: macrobf@gmail.com; Tel.: +86-27-63233058*

[b] *Engineering Research Center of Nano-Geomaterials of Ministry of Education, China University of Geosciences, Wuhan, 430074, China. E-mail: marui.cug@gmail.com; Tel.: +86-013971315390*

Natural kaoline without any further modification was used as a novel catalyst for facile green ring-opening polymerization of L-lactide.

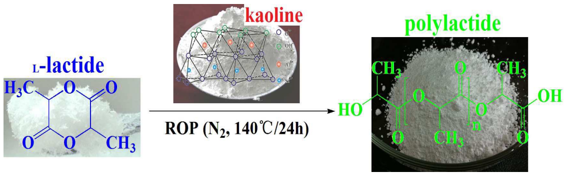

This work demonstrates a facile and green route for the solvent-free ring-opening polymerization (ROP) of L-lactide, which catalyzed by natural kaoline for the first time. PLA in 68.5% yield was obtained under the conditions of catalysis with a mass ratio of $m_{(kaoline)}/m_{(LA)}$ = 1/1500 , at 140 °C, for 24 h, resulting in high molecule weight (Mn = 4.55x 10^4 g/mol) and low polydispersity indexes (PDI = 1.34). Results from DSC and XRD revealed that the interaction between PLA chains weakened by the plasticizing effect of kaoline. The rigid structure of kaoline can prevent PLA chains from crystallizing, thus caused the glass transition temperature decreasing of the obtained PLA product. O, Si and Al were shown to be the main composition of kaoline with the exsistance of less than 2% of Ti, Fe, K, Ca, Mg by XPS and XRF. Layered structure of kaoline was examined by SEM and TEM which determines the polymer chain growth model and catalytic mechanism. XRF showed that the content of heavy metal in the product was lower than 5 ppm without removing catalyst, which well meet the requirement of medical devices. The catalytic behavior of kaoline lays the foundation of natural mineral catalyst in the field of medical aliphatic ester polymerization.

Introduction

Considerable attention has been devoted to PLA in recent years,[1-3] because of its wide range of applications on the biomedical,[4] packing,[5] and agricultural fields,[6] since it is one of the renewable and readily biodegradable resource.[7] PLA are prepared predominantly through ROP of lactide, and stannous 2-ethylhexanoate is used as the catalyst not only in commercial production but also in most scientific research until now. The tin salt shows high catalytic efficiency and excellent versatility. However, its cytotoxicity has aroused deep concern about the biosafety and its application in biomedical areas because, in practice, it is impossible to entirely remove the catalyst metal residue from the product. So, the novel catalysts with high performance and low toxicity are desirable.

The past few decades have witnessed the rapid development of metal complexes for the ROP of lactide.[8,9] Metal complexes including aluminum,[10] magnesium,[11] zinc,[12] titanium,[13] lanthanides,[14] and other metals[15,16] have been reported as excellent initiators/catalysts for the controlled ROP of lactide to afford polymers with both high Mw and low PDI. Not long ago, biomolecule derivatives such as guanidine[17] and glutamic acid[18] were used as initiators for the controlled synthesis of biodegradable PLA with high Mw and low PDI. Despite these advantages, the requirement of delicate, complicated fabrication procedure leads to a high cost for the synthesis which limits its practical use.

Recently clay minerals as natural nano-sized particles is widely used in sustainable energy, green catalysis and human healthin line with the rapid growth in nanotechnology research on synthetic materials.[19,20] Clay have long been used as catalysts and supports in organic reactions.[21-23] Since 1915, floridin was investigated for the polymerization of unsaturated compounds and a wide variety of other reactions.[24] Clay minerals including halloysite,[25] montmorillonites,[26-28] zeolite[29] and allophane[30-31] have also been reported for organic reactions.

However, there are few reports about the ROP catalyzed by clay minerals. In our previous work, palygorskite was tentatively used for ROP of ε-caprolactone.[32] Among these clay minerals, kaoline have attracted considerable attention, because of its high performance and low toxicity[33-36]. It is a 1:1 layer sheet structured hydrated aluminum silicate with siliconoxygen tetrahedral layer and one alumina octahedral layer with pseudo-hexagonal symmetry. Herein, a facile and green route for the solvent-free ROP of L-lactide catalyzed by natural kaoline without any modification was demonstrated(Fig. 1).

Experimental Section

Materials

Kaoline clay used in this experiment was procured commercially from China Minerals Processing Corporation, Tianjin, China. The sample was used without any further modification. L-lactide purchased from Esun industrial Co., Ltd, Shenzhen, China. The sample was purified by recrystallization from toluene twice before use. All the other reagents were analytical grade, which obtained from China National Pharmaceutical Group Corporation.

ROP of L-lactide catalyzed by kaoline

A typical polymerization test was by adding kaoline and L-lactide with different weight ratio (1/6000, 1/3000, 1/1500, 1/500, 1/300) into a 50 mL round-bottom flask.[15,16,32] After three vacuum/nitrogen cycles, then reacted at 120-150 °C for 8-36 h. The resulting PLA was dissolved in dichloromethane and precipitated in cold methanol.

Characterization

X-ray photoelectron spectroscopy (XPS) was carried out on a Perkin-Elmer PHI5400 ESCA. X-ray fluorescene (XRF) were done using a Quant-X of Thermofisher. Fourier transform-infrared (FT-IR) and ^{1}H nuclear magnetic resonance (^{1}H-NMR) were tested on Perkin-Elmer 983 and Varian Mecry Plus 400NB, respectively. Gel permeation chromatography (GPC) were conducted with a Shimadzu LC-20AD chromatograph.

X-ray powder diffraction (XRD) was recorded on a Rigaku Multiflex powder diffractometer. Differential scanning calorimetry (DSC) was performed using a Diamond PE calorific analyzer. Scanning electron microscopy (SEM) was conducted with a Cambridge S-250MK3 UK microscope with an acceleration voltage of 10 kV. Transmission electron microscope (TEM) was examined by a JEM-2010 microscope.

Results and discussion

The empirical formula of kaoline is $Si_2Al_2O_5(OH)_4$ (other formulas are Al_2O_3•$2SiO_2$•$2H_2O$ and $Al_2O_7Si_2$•$2H_2O$), which has a molecular weight of 258.071 g/mol. Ideal chemical structure of kaoline is a layer sheet with one siliconoxygen (SiO_4) tetrahedral layer and one alumina $[Al(O,OH)_6]$ octahedral layer (or expressed in other way, $[Si_2O_5]^{2-}$ sheet and $[Al_2(OH)_4]^{2-}$ sheet), as shown in Fig. 2. However, there are some other metals, such as Ti, Fe, K, Ca, Mg partly substituting for Si and Al in natural exist kaoline.[33] XPS and XRF were carried out to analyze the component of kaoline. The binding energies of O1s (531.8 eV), Si2p (102.5 eV), Al2p (74.6 eV) were displayed in Fig. 3. And the binding energies of Ca3p (23.5 eV), Mg2p (49.8 eV), Fe3s (98.6 eV), K2p (295.0 eV) and Ti2s (560.9 eV) revealed that less than 2% of the Si and Al has been substituted by these metals. All the data are in agreement with those reported in previous articles.[34,35] Table 1 shows the chemical compositions of kaoline by XRF. Silica and alumina are in major quantities with trace amount of other oxides such as titanium oxide, ferric oxide, potassium oxide, calcium oxide, magnesium oxide which is consistent with the results of XPS.[37]

FT-IR spectrum was conducted to provide more structural information about kaoline and PLA-3 (Fig. 4(a)). The following features are observed in the FT-IR spectra of kaoline: a broad band around 3440 cm^{-1} (O-H stretching vibrations) and an intense band at 1090 cm^{-1} (Si-O stretching vibrations), 790 cm^{-1} (Al-Mg-OH stretching vibrations), these characteristics are related to the presence of SiO_2, Al_2O_3 and MgO.[33,35,38] Compared with the FT-IR spectrum of kaoline, FT-IR spectroscopy of PLA-3 revealed the existence of -OH (3410 cm^{-1}), $-CH_3$ (2990 cm^{-1}), $-CH_2$ (2950 cm^{-1}) C=O (1750 cm^{-1}) and C-O (1080 cm^{-1}). The spectral features of PLA with other catalyst weight ratio were similar, which indicated the successful synthesis of PLA.[13,14,39] The formation of PLA/kaoline composite was demonstrated by the almost disappearance of the peak at 790 cm^{-1} of kaoline, and appearance of new peak at 750 cm^{-1}.[32] Different from conventional small molecule catalysts,[3,12,15] kaoline used here is a particle with specific morphology and size, which will influence both the microstructure and properties of the prepared PLA.

The physico-chemical properties of acid and alkaline treatment kaoline has been investigated intensively,[33,35] and it is promising to be used as adsorbent and catalyst. However, there are no reports about the catalytic polymerization of kaoline. The GPC results of PLA prepared with different weight ratio of kaoline was summarized in Table 2. The kaoline catalytic system was found to efficiently promote the ROP of L-lactide. The molecular weights (Mn and Mw) of the polymeric products were affected by the $m_{(kaoline)}/m_{(LA)}$ ratio and the maximum of molecular weight ($Mn = 4.55 \times 10^4$ or $Mw = 6.09 \times 10^4$) was achieved at $m_{(kaoline)}/m_{(LA)}$ ratio of 1/1500, which shows that lower catalyst concentration could be helpful for polymerization. The Mn and PDI data of PLA are much better to those obtained from conventional mononuclear metal complex[10,11] and biomolecule derivatives,[17,18] and similar to those obtained from multinuclear metal complexes.[12,15,16] This can be ascribed to the multinuclear metal structure of kaoline. As the increase of catalyst concentration, the PDI became larger, but it is still lower than 1.5. This due to the increase of the initiation sites with different catalytic activity, which is analogues with the ROP of L-lactide catalyzed by multinuclear metal complexes.[8,9]

In addition, other parameters such as reaction time and temperature were also investigated at the ratio of 1/1500 (Table 2). At the polymerization temperature of 140 °C (entry 3 and 6-8), the catalytic activities increased with the reaction time increased from 8 h to 24h, and well-controlled polymerization was observed from the narrow PDI (1.25-1.34). The highest Mn and conversion of the products were achieved at 24h. When the reaction time reached 36 h, the Mn and conversion decreased, which should be ascribed to transesterification caused by long reaction time.[8,32] At the polymerization time of 24h (entry 3 and 9-11), increasing temperature from 120 to 150 °C leads to the increases of monomer conversion, the Mn decreased and PDI broadened when the temperature exceeded 140 °C. This may also be attributed to the thermal depolymerization and the acceleration of transesterification as the polymerization temperature increase.[12,14,15]

Compared to PLA obtained from conventional metal complex catalysts, such as dinuclear magnesium, zinc and aluminum,[8] trinuclear and teranuclear magnesium,[9] alkaline-earth metal complexes,[12] yttrium phosphasalen,[14] Ni(II)-Sm(III)[15] and Ni(II)-Ln(III) complexes,[16] PLA prepared by kaoline have higher Mn at lower catalyst concentration. Though metal-free biomolecule derivatives such as guanidine[17] and glutamic acid[18] can act as initiators, maximum Mn (1.56×10^4 and 3.62×10^4) obtained at high initiator concentration (1/100 and 1/200). In addition, complicated fabrication procedure leads to high cost and environmental pollution for the metal complexes and biomolecule derivatives synthesis. Meaningfully, natural kaoline was used as catalyst for the ROP of L-lactide without any further modification in this work, which can simplify the preparation of catalyst and lower the cost of PLA synthesis.

^{1}H-NMR spectrum of PLA-3 (Fig. 4(b)) are assigned as follows: 1.65 ppm for methyl group and 5.36 ppm for the methine of main chain of PLA, the additional signals appearing at 2.38, 4.12 and 4.45 ppm should be assigned to the methyl, the hydroxyl and the methine of end group, respectively.[15,16] This demonstrates the successful synthesis of PLA again.

The thermal properties of PLA-3 were characterized by DSC (Fig. 4(c)). The glass transition temperature (T_g) and melting temperature of PLA-3 were 49.1°C and 135°C, respectively, which are lower than that of PLA catalyzed by small molecule catalysts.[3,12,15] This can be ascribed to the plasticizing effect caused by kaoline, which is in consistent with the results reported in previous articles.[40,41] Fig. 5(a) shows the interaction of PLA chains catalyzed by conventional small molecule catalysts, such as $SnOct_2$ and other metal complexes. Van der Waals' force and hydrogen bond between PLA chains can decrease chain mobility, and thus increase T_g.[8-11] The addition of kaoline weakened interaction between PLA chains as shown in Fig. 5(b). As a result, decreasing T_g was observed due to the increased chain mobility.[42,43] Unlike conventional oligomer plasticizer such as polyethylene glycol, big size of kaoline with rigid structure prevent the PLA chain from crystallization. The crystallinity degree of PLA catalyzed $SnOct_2$ ranged from 34.9%[44] to 62.3%[45]. However, melt enthalpy of PLA-3 indicated in DSC curves was 16.99 J/g and the crystallinity degree was 18.3% (the melt enthalpy per gram of the component in its theoretically completely crystalline state, 93 J/g). This revealed that the crystallinity of prepared PLA has already been decreased by the plasticizing effect of kaoline dramatically.

The XRD patterns of kaoline and PLA-3 are depicted in Fig. 6. The main diffraction reflections of kaoline at 2θ of 16.3°, 26.5°, 30.8° and 35.3°, are ascribed to Al_2O_3, SiO_2, Fe_2O_3 and TiO_2, respectively.[33, 38,41] As reported in literature,[39-41] only peak of 2θ = 16.6° assigned to the reflection of α-phase crystallite of PLA, which is attributed to the perfect crystalline nature of PLA. Semicrystalline property can be seen from the characteristic diffraction peaks of PLA-3 appears at 2θ = 16.6°, 18.3° and 21.7°, which is different from PLA prepared by small molecule catalysts.[3,12,15] In contrast, two new peaks appeared in the XRD patterns of PLA-3, which indicated that the crystallinity degree of PLA is altered by the present catalyst of kaoline.[42-44] This observation is in agreement with DSC results.

SEM and TEM images of kaoline and PLA-3 are shown in Fig. 7. Granular-like pattern with clear edge of kaolin mineral layers was observed in Fig. 7(a), the size of the particles ranged from 0.5 μm to 4μm.[33,46] The TEM of kaoline also shows layered structure with micron level, which was further supported the results of SEM. Stacking phenomenon was observed in the TEM image, which is common in natural minerals.[34,35] PLA-3 showed granular structure and visible on the surface of kaoline, the edge of which became sleek. Neat PLA catalyzed by small molecule catalysts[3,12,15] showed a glossy and ordered morphology without specific shape which indicated kaoline acting as template in the process of PLA-3 chains grow,[32,47] as shown in Fig. 8(a-d). The TEM of PLA-3 revealed that PLA prepared by kaoline had layered structure and well exfoliated, particle size after polymerization was slightly lower (1-3 μm), due to mechanical stir during the polymerization.[40,47]

Kaoline has a chemical structure of siliconoxygen tetrahedral layer and alumina octahedral layer, and exist Ti, Fe, K, Ca, Mg partly substituting for Si and Al, which is similar to multinuclear metal complexes.[48,49] According to the investigation reported by Ajellal,[50] when there is hydroxyl and Lewis acidic metal center on the surface of kaoline, , this ROP systems based on kaoline involves a so-called activated monomer mechanism (AMM). As it is shown in Fig. 8, the Lewis acidic metal center first activates the monomer upon coordination to its oxygen. The protic nucleophilic additive - commonly a hydroxyl compound - then initiates the polymerization upon attack of the electrophilic carbon atom of the carbonyl group, which results in the ring-opening of the heterocycle *via* oxygen-acyl bound cleavage. The hydroxyl compound co-catalyst initially introduced and hydroxy end-capped macromolecules eventually produced during the process all play the role of the nucleophile. These hydroxy end-capped molecules are involved in exchange/transfer reaction equilibria as “active” and “dormant” species, which has been demonstrated in the alkaline-earth metals (Mg, Ca, Sr, Ba)/*i*PrOH binary catalytic systems for the ROP of L-lactide.[51] As long as these transfer equilibria are rapid enough compared to the initiation and subsequent propagation steps.[12] This AMM of PLA catalyzed by kaoline differs from the previous polycaprolactone catalyzed by palygorskite.[32] In our previous work, ε-caprolactone was demonstrated to be initiated by the constituent water of palygorskite, instead of Lewis acidic metal center. The two steps of the reaction, namely, nucleophilic addition and ring-opening.

Heavy metals widely exists in our surrounding environment, such as toys, low-cost jewelry, dye and concrete composites.[52,53] It may cause disease when accumulated to a certain amount. High demands are placed on medical-grade polymers concerning their biocompatibility and chemical purity. This is the reason why the chemical purity of polymeric medical devices must be examined to ensure safe use. Table 3 shows the content of heavy metal in PLA-3 and PLA-5, which determined by XRF. The results revealed that there was no Sn and Hg exist in the PLA. The total concentration of heavy metal is 2.453 ppm for PLA-3 ($m_{(kaoline)}/m_{(LA)} = 1/1500$). When the catalyst concentration reach the maximum (1/300), the total content was also lower than 5 ppm, which is closer to the PLA fibers for medical devices.[54]

The heavy metal content of PLA catalyzed by kaoline is much lower than the limit announced in American Society for Testing and Materials (ASTM) F 1925-05, where the limit for Sn and all other heavy metal are 200 ppm and 300 ppm, respectively. The total content of heavy metal in PLA catalyzed by kaoline are much superior to medical PLA obtained from conventional $SnOct_2$.[55] Results in table 3 revealed that only the Sn content of the two samples exceeds 10 ppm, while no data of other heavy metal content is available. This PLA proved to be nontoxic with bacterial luminescence test and two protozoan assays, and applied to controlled release of ofloxacin. This suggested that PLA catalyzed by kaoline can be used in the field of medical devices.

Conclusions

In summary, kaoline can serve as an efficient catalyst for the ROP of L-lactide. PLA with high molecule weight and low polydispersity indexes can be obtained at low catalyst concentration. Different from conventional small molecule catalysts, big size kaoline with rigid structure not only plasticize PLA, but also act as template in the process of PLA chains grow. Lewis acidic metal center on the surface of kaoline can initiate L-lactide by AMM and external hydroxyl of kaoline promote the exchange/transfer and propagation reaction. Above all, the content of heavy metal in PLA was lower than 5 ppm, which is promising in field of drug carrier and medical devices.

Acknowledgments

This work was support by the Fundamental Research Funds for the Central Universities (CUGL100407, CUGL20118), the National Natural Science Foundation of China (41372367), the Natural Science Foundation of Hubei Province (2012 FFA111, 2010BFA022) and the public service project of the Chinese Ministry of Land and Resources (201311024).

References

1 M. M. Reddy, S. Vivekanandhan, M. Misra, S. K. Bhatia, A. K. Mohanty A K, *Prog. Polym. Sci.*, 2013, **38**, 1653-1689.

2 S. Slomkowski, S. Penczek, A. Duda, *Polym. Adv. Technol.,* 2014, **25**, 436-447.

3 M. Singhvi and D. Gokhale, *RSC Adv.*, 2013, **3**, 13558-13568.

4 I. Armentano, N. Bitinis, E. Fortunati, S. Mattioli, N. Rescignano, R. Verdejo, M. A. L. Manchado, J. M. Kenny J M, *Prog. Polym. Sci.*, 2013, **38**, 1720-1747.

5 J. W. Rhim, H. M. Park, C. S. Ha C S, *Prog. Polym. Sci.*, 2013, **38**, 1629-1652.

6 S. M. A. Tawakkal, M. J. Cran, J. Miltz, S. W. Bigger, *J. Food Sci.*, 2014, **79**, 1477-1490.

7 J. M. Raquez, Y. Habibi, M. Murariu, P. Dubois, *Prog. Polym. Sci.*, 2013, **38**, 1504-1542.

8 W. L. Kong, Z. X. Wang, *Dalton Trans.*, 2014, **43**, 9126-9135.

9 Y. Gao, Z. R. Dai, J. J. Zhang, X. X. Ma, N. Tang, J. C. Wu, *Inorg. Chem*. 2014, **53**, 716-726.

10 L. Postigo, M. C. Maestre, M. E. G. Mosquera, T. Cuenca, G. Jimenez, *Organometallics*, 2013, **32**, 2618-2624.

11 J. P. Davin, J. C. Buffet, T. P. Spaniol, J. Okida, *Dalton Trans.*, 2012, **41**,

12612-12618.

12 Y. Sarazin, B. Liu, T. Riosnel, L. Maron, J. F. Carpentier, *J. Am. Chem. Soc.*, 2011, **133**, 9069-9087.

13 T. K. Saha, B. Rajashekhar, D. Chakraborty, *RSC Adv.*, 2012, **2**, 307-318.

14 C. Bakewell, T. P. A. Cao, N. Long, X. F. L. Goff, A. Auffrant, C. K. Williams, *J. Am. Chem. Soc*. 2012, **134**, 20577-20580.

15 G. Q. Xiao, B. Yan, R. Ma, W. J Jin, X. Q. Lu, L. Q. Ding, C. Zeng, L. L. Chen, F. Bao, *Polym. Chem.*, 2011, **2**, 659-664.

16 L. Q. Ding, W. J. Jin, C. Zeng, L. L. Chen, X. Q. Lu, G. H. Yuan, J. R. Song, D. D. Fan, F. Bao, *Inorg. Chem. Commun*. 2011, **14**, 1274-1278.

17 H. Li, S. H. Zhang, J. P. Jiao, Z. F. Jiao, L. J. Kong, J. Xu, J. L. Li, J. Q. Zuo, X. N. Zhao, *Biomacromolecules*, 2009, **10**, 1311-1314.

18 O. T. Boullay, N. Saffon, J. P. Diehl, B. M. Vaca, D. Bourissou, *Biomacromolecules*, 2010, **11**, 1921-1929.

19 C. H. Zhou and J. Keeling, *Appl. Clay Sci.*, 2013, **74**, 3-9.

20 S. S. Ray and M. Okamoto, *Prog. Polym. Sci.*, 2003, **28**, 1539-1641.

21 G. Nagendrappa, *Appl. Clay Sci.*, 2013, **53**, 106-138.

22 C. H. Zhou., *Appl. Clay Sci.*, 2011, **53**, 85-86.

23 C. H. Zhou, *Appl. Clay Sci.*, 2011, **53**, 87-96.

24 D. M. C. Macewan, *Nature*, 1948, **162**, 195-196.

25 S. Jana and S. Das, *RSC Adv.*, 2014, **4**, 34435-34442.

26 L. Zatta, L. P. Ramos, F. Wypych, *Appl. Clay Sci.*, 2013, **80**, 236-244.

27 D. S. Tong, Y. M. Zheng,W. H. Yu , L. M. Wu, C. H. Zhou , *Appl. Clay Sci.*, 2014, **100**, 123-128.

28 A. Perez, M. Montes, R. Molina, S. Moreno, *Appl. Clay Sci.*, 2014, **95**, 18-24.

29 Y. T. Algoufi and B. H. Hameed, *Fuel Process. Technol.*, 2014, **126**, 5-11.

30 E. G. Ramirez, B. K. G. Theng, M. L. Mora, *Appl. Clay Sci.*, 2010, **47**, 182-192.

31 D. W. Lee, Y. M. Park, K. Y. Lee, *Catal. Surv. Asia*, 2009, **13**, 63-77.

32 G. Z. Wang, R. Ma, T. Chen, C. J. Yan, J. Gao, F. Bao. *Polym-Plast. Technol.*, 2013, **52**, 1193-1199.

33 A. K. Panda, B. G. Mishra, D. K. Mishra, R. K. Singh, *Colloids Surf. A: Physicochem. Eng. Asp.*, 2010, **363**, 98-104.

34 T. Juettner, H. Moertel, V. Svinka, R. Svinka, *J. Eur. Ceram. Soc.*, 2007, **27**, 1435-1441.

35 C. Belver, M. A. B. Munoz, M. A. Vicente, *Chem. Mater*. 2002, **14**, 2033-2043.

36 Y. R. Xie, L. H. Shen, J. Xiao, D. X. Xie, J. Zhu, *Energy Fuels*, 2009, **23**, 5199-5209.

37 S. S. Wang, Q. Liu, X. L. Tan, C. M. Xu, M. R. Gray, *Energy Fuels*, 2013, **27**, 2465-2473.

38 A. N. Oliverira, L. R. S. Coasta, L. H. O. Pires, L. A. S. Nascimento, R. S. Angelica, C. E. F. Costa, J. R. Zamian, G. N. R. Filho, *Fuel*, 2013, **103**, 626-631.

39 Z. Zhang, L. B. Chen, J. Gao, F. Bao, J. Yin, B. Chen, H. Wang, Y. Chen, L. Shang, *J. Polym. Eng.,* 2013, **33**, 659-664.

40 S. K. Pillai, V. Ojijo, S. S. Ray, *J. Appl. Polym. Sci.*, **2014**, DOI:

10.1002/APP.40414

41 E. Olewnik and J. Richert, *Polym. Compos.*, 2014, **35**, 1330-1337.

42 J. H. Lee and Y. G. Jeong, *Fiber. Polym*. 2011, **2**, 180-189.

43 H. G. Tian and H. Tagaya H, *J. Mater. Sci.,* 2007, **42**, 3244-3250.

44 M. X. Liu, Y. Zhang, C. R. Zhou, *Appl. Clay Sci.*, 2013, **75**, 52-59.

45 C. X. Zhang, B. Wang, Y. Chen, F. Cheng, S. C. Jiang, *Polymer*, 2012, **53**, 3900-3909.

46 W. Y. He, Q. L. Ma, J. Wang, J. Yu, W. R. Bao, H. Z. Ma, A Amrane, *Appl. Clay Sci*., 2014, **99**, 178-186.

47 S. J. P. Mclnnes, H. Thissen, N. R. Choudhury, N. H. Voelcker, *J. Colloid Interf. Sci*., 2009, **332**, 336-344.

48 M. A. Sinenkov, T. A. Glukhova, A. V. Cherkasov, A. A. Trifonov, *Russ. Chem. B+.*, 2013, **62**, 722-730.

49 M. Delferro and T. J. Marks, *Chem. Rev.*, 2011, **111**, 2450-2485.

50 N. Ajellal, J. F. Carpentier, C. Guillaume, S. M. Guillaume, M. Helou, V. Poirier, Y. Sarazin, A. Trifonov, *Dalton Trans.*, 2010, **39**, 8363-8376.

51 Y. Sarazin, V. Poirier, T. Roisnel, J. F. Carpentier, *Eur. J. Inorg. Chem.*, 2010, **22**, 3423-3428.

52 Z. Giergiczny and A. Krol, *J. Hazard. Mater.*, 2008, **160**, 247-255.

53 M. Guney, G. J. Zagury, *Environ. Sci. Technol.*, 2012, **46**, 4265-4274.

54 J. Jolanta, G. J. Karolina, G. Agnieszka, T. S. Krystyna, C. Maciej, *Fibres Text. East. Eur.*, 2012, **20**, 135-141.

55 M. Sobczak, G. N. Jawecki, W. L. Kolodziejski, P. Gos, K. Zoltowska, *Int. J. Pharm.*, 2010, **402**, 37-43.

Figure and table captions:

Fig. 1 ROP of L-lactide catalyzed by naural kaoline.

Fig. 2 crystal structure of kaoline.

Fig. 3 XPS spectra of kaoline.

Fig. 4 (a)FT-IR spectrum of the kaoline and PLA-3 ($m_{(kaoline)}/m_{(LA)} = 1/1500$). (b)^{1}H-NMR in $CDCl_3$ and (c) DSC of PLA-3.

Fig. 5 Plasticizing effect of kaoline (a) PLA catalyzed by conventional small molecule catalysts, (b) PLA catalyzed by kaoline.

Fig. 6 XRD patterns of the kaoline and PLA-3 ($m_{(kaoline)}/m_{(LA)} = 1/1500$).

Fig. 7 (a)SEM and (b)TEM of kaoline, (c)SEM and (d)TEM of PLA-3.

Fig. 8 Chain growth model and mechanism of PLA catalyzed by kaoline.

Table 1 Chemical analysis of kaoline

Table 2 L-lactide polymerization catalyzed by kaoline

Table 3 Heavy metals analysis of kaoline and PLA

Fig 1

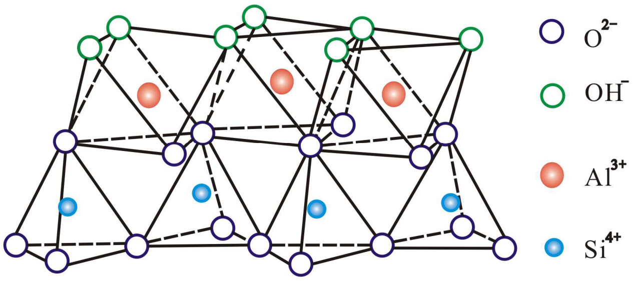

Fig. 2

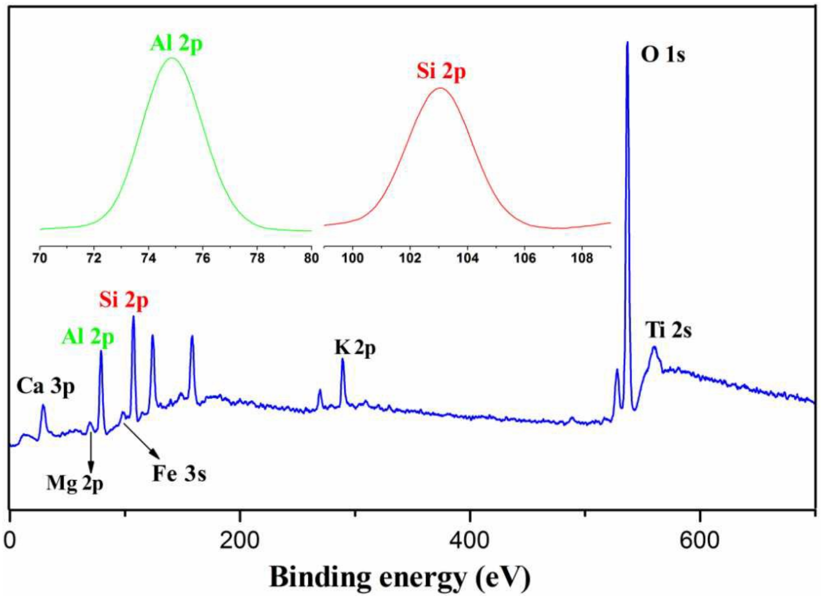
Al 2p
Si 2p
O 1s
70
72
74
76
78
80
100
102
104
106
108
Si 2p
Al 2p
Ca 3p
K 2p
Ti 2s
Mg 2p
Fe 3s
0
200
400
600
Binding energy (eV)

Fig. 3

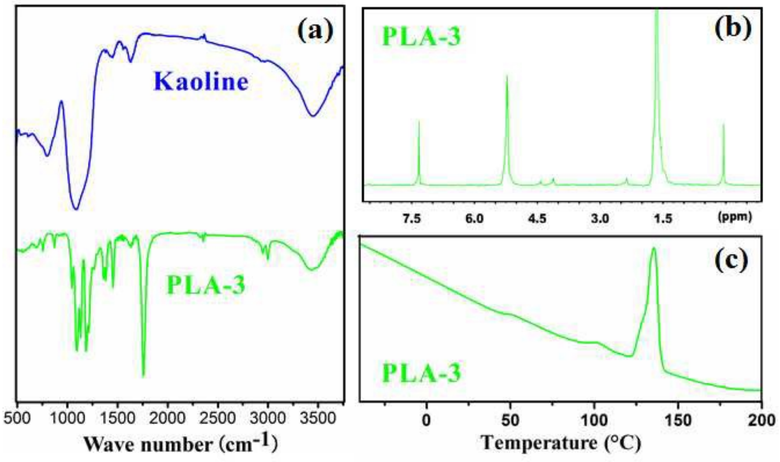
(a)
Kaoline
PLA-3
500 1000 1500 2000 2500 3000 3500
Wave number (cm-1)
(b)
PLA-3
7.5 6.0 4.5 3.0 1.5 (ppm)
(c)
PLA-3
0 50 100 150 200
Temperature (°C)

Fig. 4

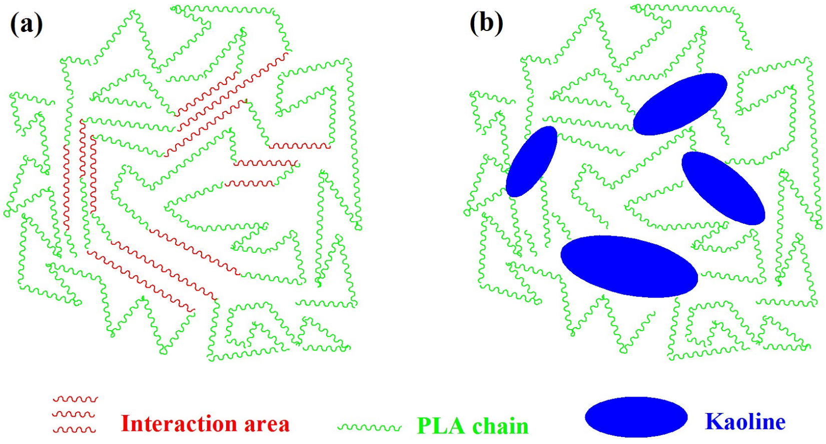

Fig. 5

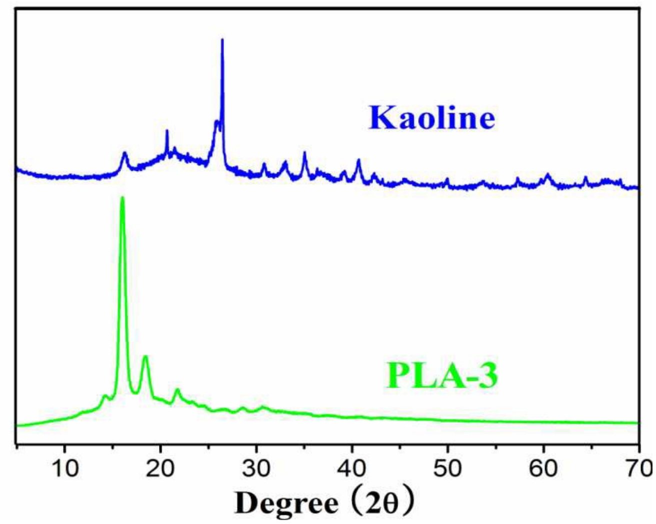

Fig. 6

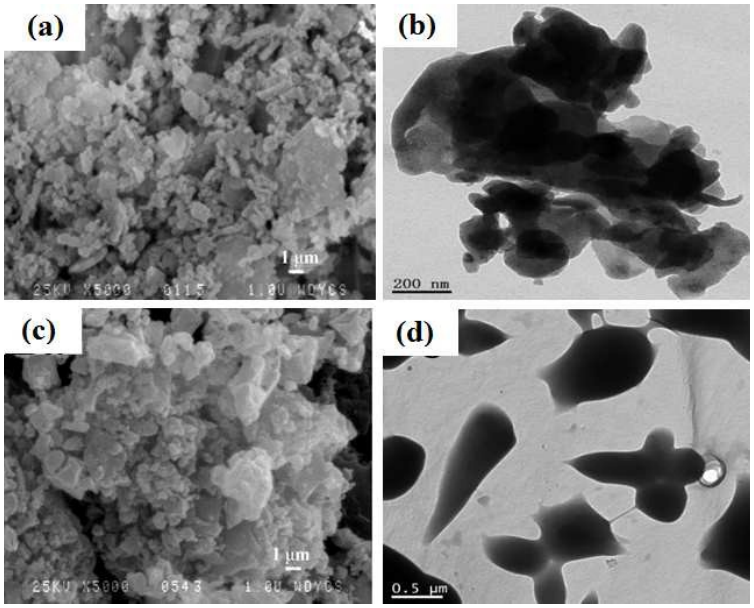
(a)
1 μm
25KV X5000 0115 1.0U NDYCS
(b)
200 nm
(c)
1 μm
25KV X5000 0543 1.0U NDYCS
(d)
0.5 μm

Fig. 7

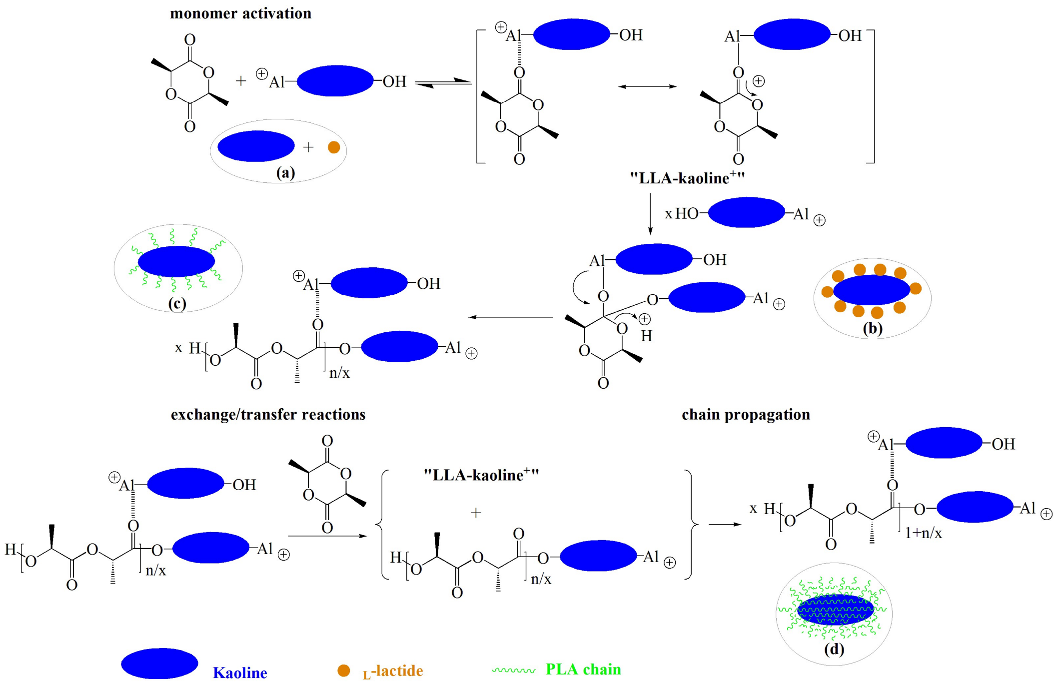
monomer activation
"LLA-kaoline⁺"
x HO—Al
(a)
(b)
(c)
(d)
exchange/transfer reactions
chain propagation
n/x
1+n/x
Kaoline
L-lactide
PLA chain

Fig. 8

Table 1

Chemicals	SiO_2	Al_2O_3	TiO_2	Fe_2O_3	K_2O	CaO	MgO
Content (wt%)	53.1	44.9	0.58	0.34	0.24	0.24	0.06

Table 2 L-lactide polymerization catalyzed by kaoline

Samples	weight ratio	t /h	T /°C	Conversion /%	Mn $/10^4$	PDI
PLA-1	1/6000	24	140	55.6	1.32	1.27
PLA-2	1/3000	24	140	60.2	2.96	1.32
PLA-3	1/1500	24	140	68.5	4.55	1.34
PLA-4	1/500	24	140	65.6	3.76	1.35
PLA-5	1/300	24	140	67.4	3.71	1.38
PLA-6	1/1500	8	140	32.0	2.34	1.25
PLA-7	1/1500	12	140	37.9	2.60	1.31
PLA-8	1/1500	36	140	65.4	4.21	1.36
PLA-9	1/1500	24	120	52.6	0.43	1.20
PLA-10	1/1500	24	130	56.7	2.62	1.28
PLA-11	1/1500	24	150	73.1	3.39	1.48

"t" represent for reaction time and "T" represent for reaction temperature.

Table 3 Heavy metals analysis of kaoline and PLA

Materials	Content (ppm)					Total
	Sn	Hg	Cr	Cd	Pb	(ppm)
PLA-3	-	-	0.375	1.680	0.398	2.453
PLA-5	-	-	1.409	2.471	1.086	4.966
LLA/PEG/$SnOct_2$[55]	14	/[a]	/	/	/	/
LLA/PET/$SnOct_2$[55]	12	/	/	/	/	/

[a] No data of Hg, Cr, Cd and Pb content is available.